# Towards the true rotation of a rigid Eurasia

Halfdan Pascal Kierulf [*], Hans-Peter Plag, Oddgeir Kristiansen, Torbjørn Nørbech
Norwegian Mapping Authority, Kartverksveien, N-3511 Hønefoss, Norway

**Abstract**

Application of space-geodetic techniques to the studies of regional intra-plate deformations requires to eliminate the rigid plate motion from the observations. In many cases, this is achieved by either using a global model for plate motion or by determining the site displacements relative to one or several sites assumed to be moving rigidly with the plate. In both cases, the resulting intra-plate motion may be biased. Here we present a new approach to the determination of the rigid plate motion for Europe. Using models to account for known intra-plate motions, a large number of site velocities is used to determine a rotation vector describing the rigid plate motion. This vector is largely unbiased by regional intra-plate deformations such as post-glacial rebound. The resulting rotation vector for Europe appears to be in between the NUVEL-1A-NNR vector and the rotation vector recently adopted by EUREF commission for the European regional reference frame.

## 1 Introduction

Space-geodetic techniques are increasingly used for geodynamical studies on regional scale. These techniques allow to determine site motions with respect to a global reference frame with accuracies down to the 1 mm/yr level. For scientific and practical purposes, it is often desired to remove the velocity field due to the rigid motion of a tectonic plate from the observations and thus to keep the average velocities for sites on that plate small. This can be achieved by fixing a regional reference frame to the ”stable part” of the plate.

Geodetic reference systems are commonly realized by a set of points for which initial epoch coordinates and (optional) linear velocities are given (see, e.g Altamimi & Boucher, 2002). As shown recently by Nocquet et al. (2001), particular care needs to be taken when fixing regional reference frames to the ”stable” part of a tectonic plate, as the identification or selection of the ”stable” part determines the relative station velocities with respect to the reference frame. Thus, a subsequent geophysical interpretation of the velocities relative to this regional frame may be affect by the specific selection of the ”stable” part since parts of the surface motion due to a given geophysical process may be absorbed in the reference frame itself.

For Europe, a regional reference frame is maintained by the IAG Subcommission EUREF. Up to 2001, the rigid motion of Eurasia was accounted for in the realizations of the ETRS89 by the motion predicted by NUVEL-1A-NNR (DeMets et al., 1994).

In the cause of the determination of ITRF2000, Altamimi & Boucher (2002) (see also Boucher & Altamimi, 2001) determined transformation between ITRF2000 and ETRF89. This new rotation vector is significantly different from the one in NUVEL-1A-NNR, thus indicating either the inadequacy

[*]phone: +47-32118100, fax: +47-32118101, Email: halfdan.kierulf@statkart.no

of the NUVEL-1A-NNR rotation or problems with the determination of the new rotation vector by Altamimi & Boucher (2002). It is important to point out that Altamimi & Boucher (2002) used

$$\vec{R} \times \vec{X} = \vec{V} \tag{1}$$

to determine the rotation vector $\vec{R}$ for Europa on the basis of 19 selected ITRF stations with presumably high geodetic quality. Here, $\vec{X}$ and $\vec{V}$ are the position and velocity, respectively.

Eq. 1 can be written in Cartesian coordinates as

$$\Omega \vec{X} = \vec{V} \tag{2}$$

where

$$\Omega = \begin{pmatrix} 0 & -r_z & r_y \\ r_z & 0 & -r_x \\ -r_y & r_x & 0 \end{pmatrix} \tag{3}$$

is the Euler matrix.

The local vertical component of the velocity vector is strongly affected by small scale phenomena and, moreover, less accurately determined than the horizontal components. Therefore, for the determination of $\vec{R}$, the local vertical component of the velocity is assumed to be zero in order to avoid a contamination of the rotation pole.

Altamimi & Boucher (2002) used station in the stable part of Eurasia with velocity residuals less than 3 mm/yr thus excluding all sites on the Eurasian plate located in Asia. Therefore, station distribution is such that the new pole is more representative for western Europe than the whole Eurasian plate.

Plag et al. (2002) pointed out that the station distribution in Scandinavia may have resulted in a large part of the expected horizontal movement due to post-glacial rebound being absorbed in the new rotation vector. They suggest that it may be more appropriate to use

$$\Omega \vec{X} + \gamma \vec{V}_{\mathrm{pgs}} = \vec{V} \tag{4}$$

for the determine of the rotation pole for Eurasia, where $\vec{V}_{\mathrm{pgs}}$ is the horizontal velocity predicted by a geophysical post-glacial model. They introduced $\gamma$ as an unknown scale factor to account for uncertainties in the model used. Here we test the hypothesis that a slightly modified version of Eq. 4 allows a better determination of the rotation pole for the rigid part of Europe.

## 2 Methodology

Secular site velocities are often determined from time series of coordinate variations (e.g. from GPS) or in analyses of a large data set covering several years (e.g. VLBI). In both cases, the actual station motion due to geophysical processes acting and many different time scales needs to be taken into account in order to get the best estimate for the secular velocity. The IERS Conventions (see McCarthy, 1996) give recommendations on how to model the motion of an observation point caused by geophysical processes in space-geodetic analyses. The list includes:

- Earth tide;
- ocean tidal loading;
- deformation due to polar movement;

- deformation due to atmospheric loading;

- post-glacial deformations;

- plate tectonics.

Not included are hydrological and cryospheric loading, deformation induced by sedimentation processes, deformation due to ground water and oil/gas extraction, neo-tectonics. The boundary between what is recommended to be modeled and what not appears to be between known and unknown processes. Thus the aim appears to be to create station coordinates that, after having taken into account all known variations, show the least variations over time. In most analyses, however, the resulting velocities still contain the secular signal due to post-glacial rebound, long-period loading and tectonics. Particularly in northern Europe, the most prominent secular contribution to intra-plate deformations is the post glacial signal.

Using Eq. 2 to determine a rotation pole for the rigid plate motion from these velocities will result in a pole affected by the other secular signals. Contamination of the rotation pole can be reduced by including model predictions for known processes in the equation. We therefore extend Eq. 2 to

$$\Omega\vec{X} + \sum_i \vec{V}_i^{\mathrm{geo}} = \vec{V}, \tag{5}$$

where $\sum_i \vec{V}_i^{\mathrm{geo}}$ describes all geophysical contributions to intra-plate deformation.

For Europe, the most important geophysical signal to be included is the post glacial rebound. For northern Europe, geophysical models predict horizontal velocities of the order of 3 mm/yr away from the former center of the ice load (Figure 1). However, this model also predicts a north component of about 0.8 mm/yr in regions of Eurasia assumed to be not influenced by the post-glacial rebound. In order to account for this deficiency of the model, we introduce a velocity offset $\delta$ in the north component in addition to the scale factor introduced by Plag et al. (2002). Restricting the model to the local horizontal components, we get

$$\vec{V}'_{\mathrm{PGS}} = \begin{pmatrix} V'^{e}_{\mathrm{PGS}} \\ V'^{n}_{\mathrm{PGS}} \end{pmatrix} = \begin{pmatrix} \gamma V^{e}_{\mathrm{PGS}} \\ \gamma V^{n}_{\mathrm{PGS}} + \delta \end{pmatrix}, \tag{6}$$

where $V_{\mathrm{PGS}}$ is the present-day velocity predicted by the post-glacial rebound model.

Using

$$\vec{V}_{en} = \Phi' \vec{V}_{xyz}, \tag{7}$$

where $\Phi'$ is the standard transformation matrix from Cartesian to local coordinates restricted to the horizontal components, we can describe the velocity model for Eurasia as

$$\Phi'(\Omega\vec{X}) + \vec{V}'_{\mathrm{PGS}} = \Phi'\vec{V}. \tag{8}$$

Table 1: Characteristic parameters of the post-glacial rebound model by Milne et al. (1999).

| | |
|---|---|
| lithospheric thickness | 120 km |
| upper mantle viscosity | $1 \cdot 10^{21}$ Pas |
| lower mantle viscosity | $5 \cdot 10^{21}$ Pas |
| earth model | PREM |
| ice model | ICE-3G |

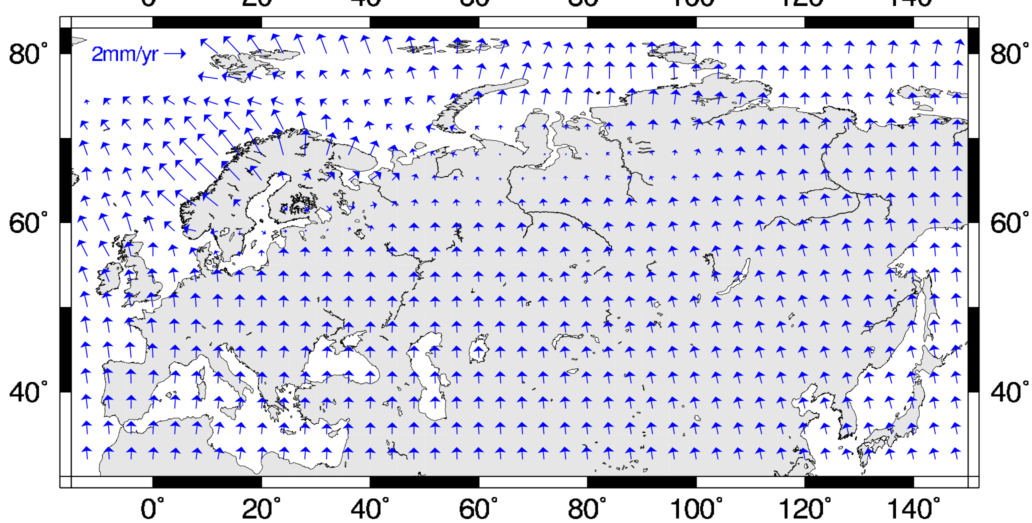


Figure 1: Horizontal velocities due to post-glacial rebound.
*The arrows indicate the horizontal velocities predicted by a typical geophysical model (Milne et al., 1999). The key parameters of the model are given in Table 1.*

# 3 Observations

The International Terrestrial Reference System (ITRS) is realized through a reference frame of a set of points, for which coordinates and secular velocities are given. The latest and most precise realization is the ITRF2000, which includes 125 sites on the Eurasian plate. From this catalogue, we have selected all GPS and VLBI sites which are not in known tectonically active regions of Eurasia, in all 77 sites. For Norway, the catalog includes only 2 points. Therefore, we have augmented the set with coordinates and velocities of 9 selected Norwegian permanent GPS stations.

The data from the Norwegian sites are analyzed with Gipsy-OasisII in the precise point positioning approach (Zumberge et al., 1997) using JPL satellite orbits and clocks as well as EOPs in a non-fiducial solution, which is converted to ITRF2000 using JPL transformation parameters.

All stations used and their velocities are plotted in Figure 2. To a large extent, the velocity map is consistent with the rigid plate motion predicted by the NUVEL-1A-NNR model. However, some regions display minor deviations from this motion indicating some intra-plate motion.

# 4 Results

The unknown rotation parameters $r_x$, $r_y$ and $r_z$, and the PGS modification parameters, factor $\gamma$ and offset $\delta$ are determined in a weighted LSQ fit of Eq. 8 to the observed ITRF2000 velocities of the sites shown in Figure 2.

The resulting scale factor and offset for the PGS-model are given in Table 2. The scale factor of $\gamma = 0.620$, indicates that the horizontal velocities predicted by the model are too large. This result is consistent with another study, where the present-day sea level trend predicted by the post-glacial model is fitted to the global tide gauge data set (Plag & Jüttner, 2001). Here, too, a scaling factor is introduced and for a large suite of models, the factor consistently turns out to be of the order of 0.8.

The offset $\delta = -0.4$ mm/yr for the north component may indicate a problem in post-glacial rebound model. Tests without the offset consistently result in much poorer fit to the observed velocities.

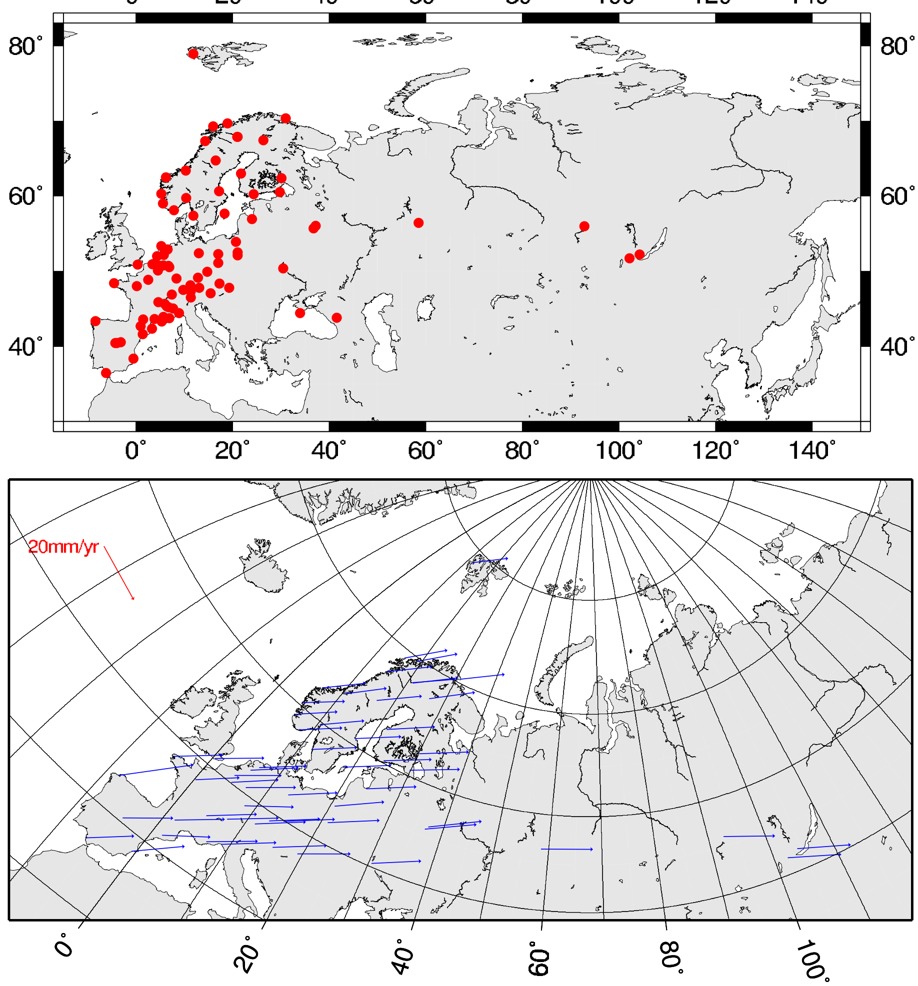


Figure 2: Distribution of observation sites.
*Upper plot: distribution of the sites selected from the ITRF2000 catalogue and additional Norwegian permanent GPS stations. Lower plot: horizontal velocities in ITRF2000. Note that the velocity map is drawn in an oblique Mercator projection with central line going through the rotation pole given for the NUVEL-1A-NNR model. In this projection, a velocity field consistent with the NUVEL-1A-NNR rigid plate rotation would be shown as parallel vectors.*

The rotation parameters resulting from the fit of Eq. 8 to the observed velocities are given in Table 3 together with the rotation parameter for NUVEL-1A-NNR and the new EUREF rotation vector. The decontaminated rotation vector for Eurasia (denote here as EURASIA) appears to be significantly different from both the NUVEL and the EUREF vectors.

Table 2: Scale factor and north offset for the post-glacial rebound model.

| |
|---|
| $\gamma = 0.620 \pm 0.105$ |
| $\delta = -0.4 \pm 0.3$ mm/yr |

The difference between the EUREF and the EURASIA vector may be caused by the station selection. To study the dependency of the rotation vector both on the site selection and the model equation, both Eq. 8 and Eq. 1 were fitted to the velocities of different subgroups of the ITRF2000 stations. For that, Eurasia was splitted into four regions, namely Central Europe, Asia, Scandinavia and the Baltic area including Finland. The rotation parameters for Eurasia were then computed for combination of

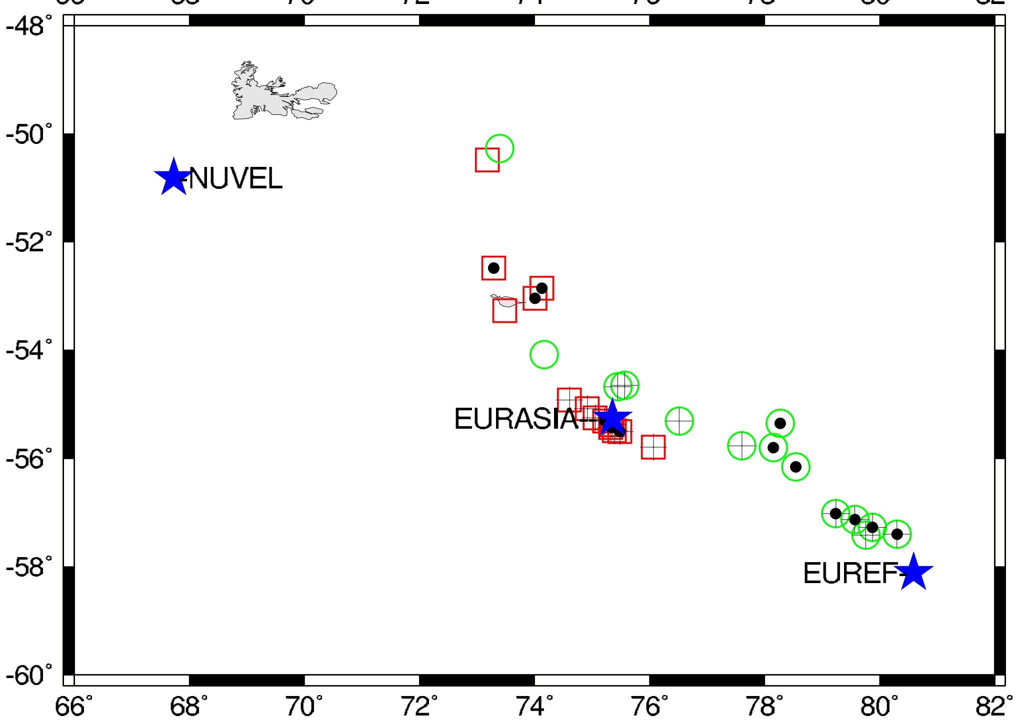


Figure 3: Geographical distribution of the rotation poles.
*Rotation poles are marked with green circles for the classical approach (Eq. 1) and red boxes for the extended velocity model (Eg. 8). Black crosses are used when the selected stations includes Central Europe and black circles are used when the selected stations includes Scandinavia.*

different regions both for the classical equation and the extended velocity model. Figure 3 shows the geographical location of the different poles. The NUVEL and EUREF poles are the two extreme locations while all other poles have an intermediate location. The EURASIA pole is in the middle between these two extremes.

Fitting Eq. 8 to any of the subsets and combinations of these results in a pole position between the two extreme poles (red boxes in Figure 3). The same is true for all poles determined here using the classical Eq. 1 (green circles in Figure 3). However, for any given subset, there is a marked difference between the results from these two equations indicating the large bias in the rigid plate rotation vector if the post-glacial rebound signal is not taken into account properly. Moreover, for the classical approach, the rotation vector depends strongly on the subset of sites while using the extended velocity model results in a rotation vector almost insensitive to the site selection.

As an example, we consider the subset of sites in Central Europe and Asia. For these stations, the classical approach results in a rotation vector $\vec{R} = (0.130, 0.506, 0.731)$ mas/yr while the extended

Table 3: Rotation parameters.

| | $r_x$ (mas/yr) | $r_y$ (mas/yr) | $r_z$ (mas/yr) |
|---|---|---|---|
| NUVEL | $0.20$ | $0.50$ | $-0.65$ |
| EUREF | $0.081 \pm 0.021$ | $0.489 \pm 0.008$ | $-0.792 \pm 0.026$ |
| EURASIA | $0.129 \pm 0.008$ | $0.494 \pm 0.010$ | $-0.732 \pm 0.009$ |

velocity model gives $\vec{R} = (0.134, 0.496, 0.731)$ mas/yr. Excluding the Asian stations and including instead the Scandinavian stations gives with the extended model almost the same rotation parameters, i.e. $\vec{R} = (0.127, 0.492, 0.735)$ mas/yr, while for the classical approach the parameters change considerably to $\vec{R} = (0.085, 0.495, 0.780)$ mas/yr. The extreme positions of the NUVEL and EUREF poles indict that on the one hand, the NUVEL-1A-NNR rotation vector for the Eurasian plate is not fully consistent with the observed velocity field in Eurasia. On the other hand, it can be concluded that the 19 stations selected by Altamimi & Boucher (2002) for the determination of the new EUREF rotation vector are neither representative for the rigid plate rotation of the European part of the Eurasian plate nor the total Eurasian plate.

In Table 4, statistical parameters are given for the residual velocities for different subsets of sites for the NUVEL and EUREF rotation vectors using the classical velocity model and for the extended model. For all subsets of sites, the extended model gives a better approximation of the observed velocity field than the classical approach.

The new approach gives a good approximation in all regions and components, except the north component in Asia. For NUVEL-NNR-1A we have clear west signal in Scandinavia (about 1.6 mm/yr) and a north signal for the hole Europe (about 0.9 mm/yr). The EUREF model gives residuals at the same level as the new approach in Scandinavia and slightly worse in continental Europe, but the EUREF model have problems in Asia.

Table 4: Weighted RMS and weighted mean of residual velocities.

*The first column gives the weighted root mean square values for the residuals for the different models in the different regions. Columns two and three give the weighted mean of the East and North components, respectively.*

| | WRMS mm/yr | WM east mm/yr | WM north mm/yr |
|---|---|---|---|
| SCANDINAVIA | | | |
| NUVEL | 1.8 | -1.6 | 0.9 |
| EUREF | 0.6 | -0.2 | 0.1 |
| EURASIA+PGS’ | 0.5 | -0.2 | 0.0 |
| ASIA | | | |
| NUVEL | 1.4 | 1.3 | 0.5 |
| EUREF | 2.0 | -1.3 | -3.0 |
| EURASIA+PGS’ | 1.0 | -0.1 | -1.8 |
| C. EUROPE | | | |
| NUVEL | 0.7 | 0.0 | 0.8 |
| EUREF | 0.5 | -0.2 | 0.3 |
| EURASIA+PGS’ | 0.5 | 0.0 | 0.1 |
| EURASIA | | | |
| NUVEL | 1.1 | -0.4 | 0.8 |
| EUREF | 0.6 | -0.2 | 0.1 |
| EURASIA+PGS’ | 0.5 | -0.1 | 0.0 |

$$\mathrm{WRMS} = \sqrt{\frac{\sum_{\mathrm{i}} \left( \frac{\mathrm{V}^{\mathrm{i}}_{\mathrm{itrf00}} - \mathrm{V}^{\mathrm{i}}_{\mathrm{model}}}{\sigma^{\mathrm{i}}_{\mathrm{itrf00}}} \right)^2}{\sum_{\mathrm{i}} \left( \frac{1}{\sigma^{\mathrm{i}}_{\mathrm{itrf00}}} \right)^2}} \qquad \mathrm{WM} = \frac{\sum_{\mathrm{i}} \frac{\mathrm{V}^{\mathrm{i}}_{\mathrm{itrf00}} - \mathrm{V}^{\mathrm{i}}_{\mathrm{model}}}{\sigma^{\mathrm{i}}_{\mathrm{itrf00}}}}{\sum_{\mathrm{i}} \frac{1}{\sigma^{\mathrm{i}}_{\mathrm{itrf00}}}}$$

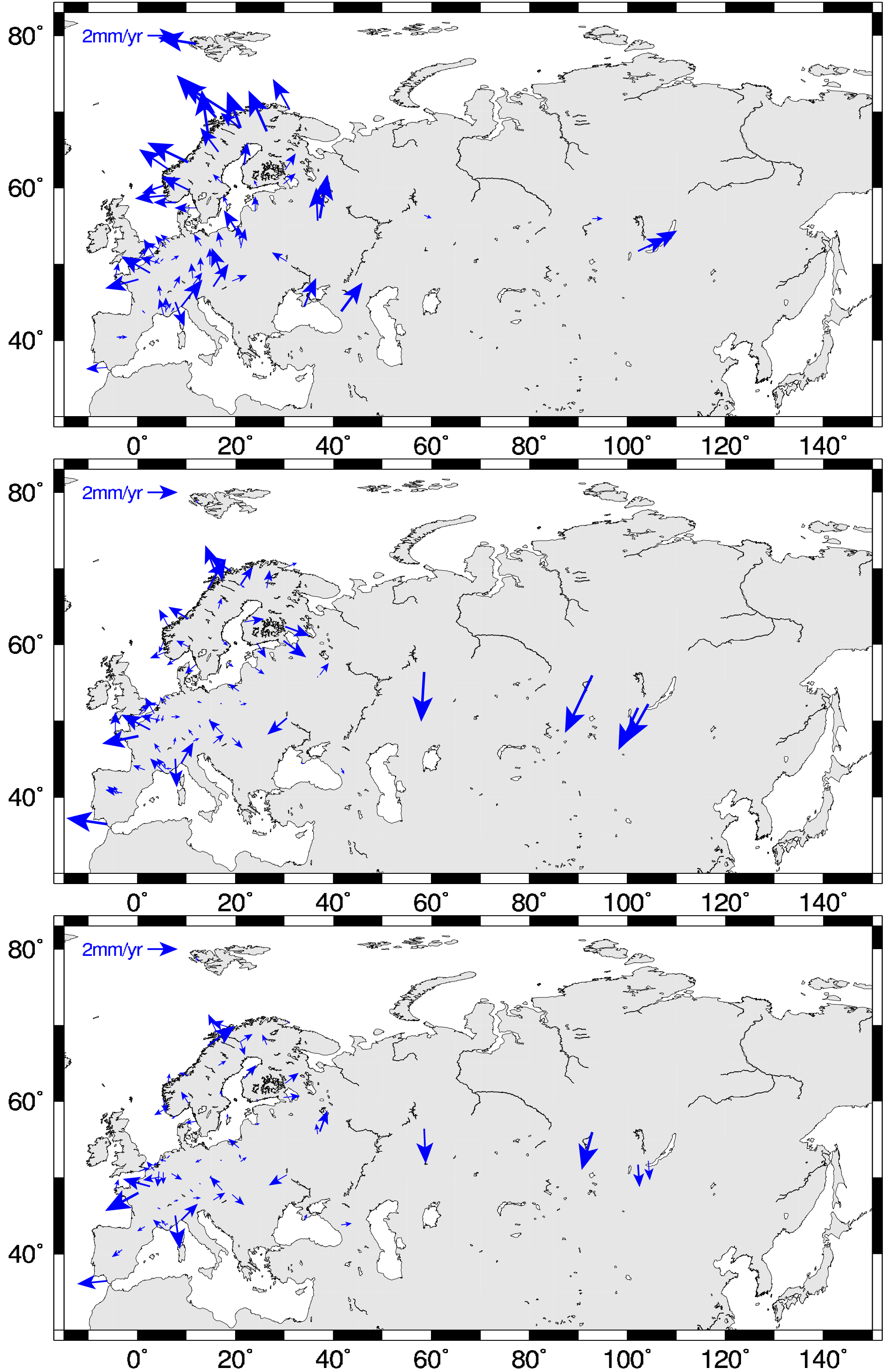


Figure 4: Residual velocities for Eurasia

*The residual velocities are the ITRF2000 velocities minus the velocities predicted by the model. Upper diagram: residuals using the NUVEL rotation vector (DeMets et al., 1994). Middle: residuals using the EUREF rotation vector (Altamimi & Boucher, 2002). Lower: residuals using the extended model determined in the present study.*

This rotation is removed by both the EUREF and the EURASIA pole. For European sites, the EURASIA pole results in slightly smaller residuals, particularly for the Scandinavian sites. For the Asian sites, the EUREF pole results in rather large residuals thus indicating that the EUREF pole only applies to the European part In Figure 4, the residual velocities for the ITRF sites included in the fit are shown for the NUVEL, EUREF and EURASIA pole. For the NUVEL-1A-NNR pole, a residual rotation is visible for all European sites. This rotation is removed by both the EUREF and the EURASIA pole. For European sites, the EURASIA pole results in slightly smaller residuals, particularly for the Scandinavian sites. For the Asian sites, the EUREF pole results in rather large residuals thus indicating that the EUREF pole only applies to the European part of the Eurasian plate.

# 5 Conclusion

We have demonstrated that the determination of the rigid plate motion vector from observed secular site velocities can be improved by including geophysical models for known processes causing secular intra-plate deformation into the model describing the velocity field. Introducing a geophysical model for post-glacial rebound in the velocity model used to determine the rotation vector of the rigid plate results in a rotation vector which to a large extent is independent of the site selection. In summary, the extended model used in this study results in

- a rotation model less dependent on the sites selected;
- a rotation model closer to the true rigid motion;
- a validation of the PGS-model;
- a modification of the PGS-model by a factor and offset in the north component;
- a residual signal better suited for further studies of intra-plate deformations;
- an improved velocity approximation of the observed velocities in all parts of Eurasia.

# References

Altamimi, Z. & Boucher, C., 2002. The ITRS and ETRS89 relationship: new results from ITRF2000, in *EUREF Publication No. 10*, edited by J. A. Torres & H. Hornik, pp. ???–???, Verlag des Bundesamtes für Kartographie und Geodäsie, Frankfurt am Main.

Boucher, C. & Altamimi, Z., 2001. Memo: Specifications for reference frame fixing in the analysis of a EUREF GPS campaign, Unpublished memo available at http://lareg.ensg.ign.fr/EUREF/.

DeMets, C., Gordon, R. G., Argus, D. F., & Stein, S., 1994. Effect of recent revisions to the geomagnetic reversal time scale on estimates of current plate motions, *Geophys. Res. Lett.*, **21**, 2191–2194.

McCarthy, D. D., 1996. *IERS Conventions 1996*, IERS Technical Note 21, Observatoire de Paris, 95 pages.

Milne, G. A., Mitrovica, J. X., & Davis, J. L., 1999. Near-field hydro-isostasy: the implementation of a revised sea-level equation, *Geophys. J. Int.*, **139**, 464–482.

Nocquet, J.-M., Calais, E., Alamimi, Z., Sillard, P., & Boucher, C., 2001. Intraplate deformation in western Europe deduced from an analysis of the International Terrestrial Reference Frame 1997 (UTRF) velocity field, *J. Geophys. Res.*, **106**, 11,239–11,257.

Plag, H.-P. & Jüttner, H.-U., 2001. Inversion of global tide gauge data for present-day ice load changes, in *Proceed. Second Int. Symp. on Environmental research in the Arctic and Fifth Ny-Ålesund Scientific Seminar*, edited by T. Yamanouchi, no. Special Issue, No. 54 in Memoirs of the National Institute of Polar research, pp. 301–317.

Plag, H.-P., Nørbech, T., & Kristiansen, O., 2002. Effects of intraplate deformations on fixing regional reference frames, in *EUREF Publication No. 10*, edited by J. A. Torres & H. Hornik, pp. 118–124, Verlag des Bundesamtes für Kartographie und Geodäsie, Frankfurt am Main.

Zumberge, J. F., Heflin, M. B., Jefferson, D. C., & Watkins, M. M., 1997. Precise point positioning for the efficient and robust analysis of GPS data from large networks, *J. Geophys. Res.*, **102**, 5005–50017.